

Three-Level DC/DC Converter for High Input Voltage to low output voltage Adopting Symmetrical Duty Cycle Control

P. Vijay¹, Dr. J. Namratha Manohar²

¹*M.Tech student, EEE, Lords Institute of Engineering and Technology, Hyderabad, India.*

²*Professor, EEE, Lords Institute of Engineering and Technology, Hyderabad, India.*

Abstract— The recent growth of battery powered applications and low voltage storage elements are increasing the demand of efficient step-up dc-dc converters. Typical applications are embedded systems, renewable energy systems, fuel cells, mobility applications and uninterrupted power supply (UPS). These applications demand high step-up static gain, high efficiency and reduced weight, volume and cost. Some classical converters with magnetic coupling as fly-back or current-fed push-pull converter can easily achieve high step-up voltage gain. However, the power transformer volume is a problem for the development of a compact converter. The energy of the transformer leakage inductance can produce high voltage stress, increases the switching losses and the electromagnetic interference (EMI) problems, reducing the converter efficiency. Half-bridge three-level (TL) converter is a potential topology in high input voltage applications. It is essentially derived from the neutral point clamped (NPC) inverter, which can reduce the voltage stress of the power switches to only a half of the input voltage, when compared with traditional topologies. The common features of TPTL (three-phase three level) dc/dc are the employment of an NPC inverter configuration and a three-phase transformer; although the voltage stress on switches can be reduced, the numerous power switches result in the higher overall cost and increased control circuit complexity. To simplify the circuit configuration, a novel TPTL converter is proposed in this project, which keeps the advantages of the available TPTL converters including the lower voltage stress, efficient utilization for transformer, and reduced output filter requirement. The proposed concept is verified by using Matlab/Simulink software and the corresponding results are presented.

Index Terms- Three phase three levels (TPTL), Three levels, Symmetrical Duty Cycle Control, DC/DC Converter.

I. INTRODUCTION

Full-bridge dc/dc converters shown in fig.1 have been used widely in the medium-to-high power applications for the pulse control, soft-switching characteristics, and lower power rating on switches. With the proposed three-phase architecture, the converters have the superior features including lower current rating of switches, reduced input and output current ripple allowing small-size filter requirement, and better utilization of transformer core since it can comply with the aforementioned standard with simplicity, efficiency, reliability and low cost. However, in order to reduce the harmonic distortion in the three-phase boost rectifier, its output voltage has to be significantly increased with respect to the input voltage. Therefore, this increment in the output voltage also increases the voltage stress across the devices in the DC/DC step-down second stage converter. At this power level (6 kW), the DC/DC second stage converter is usually implemented with a full-bridge topology. In this case, each switch in the full-bridge topology is subjected to the full bus voltage. In this voltage range, MOSFET devices with a high r_{ds} may be used. This approach increases the conduction losses of the DC/DC converter. Another option at this power range is to use IGBT devices. However, in this case the switching frequency must be reduced and consequently the power density of the converter.

Although predominant characteristics are presented in three-phase full-bridge converters, soft switching has not been achieved which limits the switching frequency and the power density. Some solutions use three-phase resonant converters where soft-switching can be achieved, including the *LCC*-type resonant converter and *LCL*-type

resonant converter. The improved resonant converter features narrow variation in switching frequency for power control, zero voltage-switching (ZVS) realization under wide load range, and higher conversion efficiency. However, the number of power components and also the overall volume of converter are increased due to the addition of numerous passive power elements. Other alternative solutions are the non-resonant soft-switching three-phase converters. The use of asymmetrical duty cycle in the three-phase dc/dc converter was proposed, in order to obtain ZVS commutation for all switches in a wide load range. Nevertheless, the resulting topology suffers conduction losses in the rectifier stage for two series diodes conduct the load current at any time. Therefore, a three-phase version of hybrid rectifier was introduced instead of conventional three-phase rectifier; although the output inductors' volume increases, the efficiency improvement provides an overall reduction of the converter volume. This paper presents a novel Zero Voltage Switching Three-Level DC/DC converter, whose main characteristics are to reduce the voltage stress across the main switches, provide ZVS operation for all switches, and simplify the control by using the well-known phase-shift control.

This paper will first address the operation and analysis of the proposed converter. Half-bridge three-level (TL) converter is a potential topology in high input voltage applications. It is essentially derived from the neutral point clamped (NPC) inverter, which can reduce the voltage stress of the power switches to only a half of the input voltage, when compared with traditional topologies. It can also achieve ZVS easily via using the leakage inductance of the transformer and the intrinsic capacitors of the switches without additional components. To incorporate the advantages of half-bridge TL converter and three-phase full-bridge converter, three-phase three-level (TPTL) dc/dc converters were proposed. The proposed converters are composed of an NPC inverter connected to the primary side of a three-phase high-frequency transformer. The secondary side of the transformer feeds a three-phase rectifier, and the output stage of the converter is composed of the output filter and the load. The symmetrical duty cycle control was adopted in the converter proposed, and the converter has the features including lower voltage stress on switches, soft-switching capabilities, and voltage source characteristic for output stage.

A phase-shifted pulse control strategy was introduced into the converter; as a result, the switches can achieve ZVS and Zero-current-switching without additional auxiliary components. The common features of TPTL dc/dc converters mentioned previously are the employment of an NPC inverter configuration and a three-phase transformer; although the voltage stress on switches can be reduced, the numerous power switches result in the higher overall cost and increased control circuit complexity.

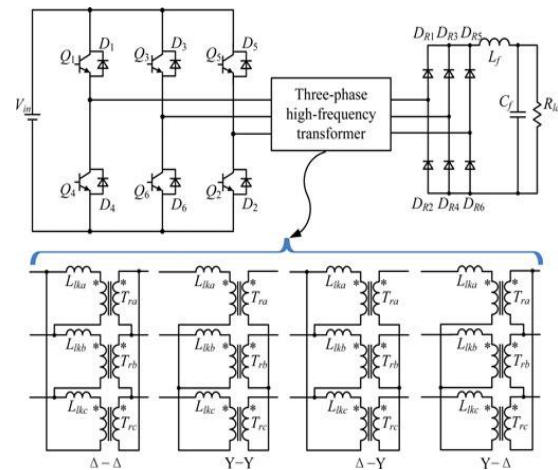


Fig.1. Circuit configuration of a three-phase full-bridge dc/dc converter.

To simplify the circuit configuration, a novel TPTL converter is proposed in this paper, which keeps the advantages of the available TPTL converters including the lower voltage stress, efficient utilization for transformer, and reduced output filter requirement; meanwhile, the number of switches is reduced significantly, along with the gate drivers and pulse channels, resulting in a simpler architecture and lower cost. In this paper, the derivation of the proposed converter is illustrated; the operation principle and the theoretical analysis are presented.

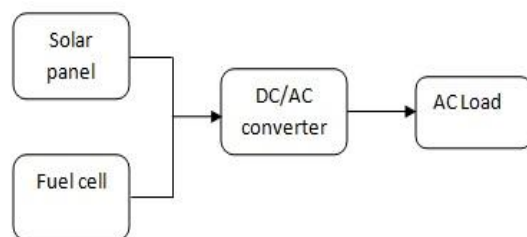


Fig.2. Block diagram representation of Renewable energy system

This Renewable energy system consists of three main parts which are PV module, balance of system and load. The major balance of system components in this systems are charger, battery and inverter. The Block diagram of the system is shown in Fig.2.

A Photovoltaic cell is basically a semiconductor diode whose p-n junction is exposed to light. Photovoltaic cells are made of several types of semiconductors using different manufacturing processes.

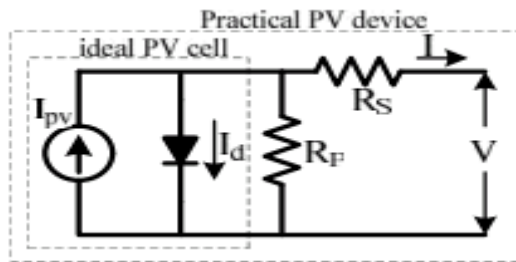


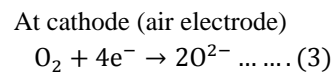
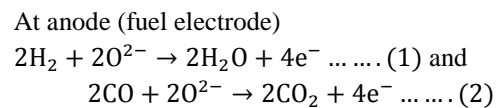
Fig.3. Practical PV device

The incidence of light on the cell generates charge carriers that originate an electric current if the cell is short circuited. The equivalent circuit of PV cell is shown in the fig.3. In the figure the PV cell is represented by a current source in parallel with diode. R_s and R_p represent series and parallel resistance respectively. The output current and voltage from PV cell are represented by I and V .

A fuel cell (SOFC) generates electrical power by continuously converting chemical energy of a fuel into electrical energy through an electrochemical reaction. The fuel cell itself has no moving parts, making it quiet and reliable. Fuel cells typically utilize hydrogen as the fuel and oxygen (usually from air) as the oxidant in the electrochemical reaction. It generates electricity, and its by-products are water and heat. Its Schematic diagram is shown in fig.4.

Fuel cells are electro-chemical devices which are used to convert the chemical energy of a gaseous fuel directly into electricity. In fuel cells, a chemical reaction takes place to convert hydrogen and oxygen into water, releasing electrons in the process. In other words, that hydrogen fuel is burnt in a simple reaction to produce electric current and water. A fuel cell consists of two electrodes, known as anode and cathode that are separated by an electrolyte is shown in Fig. 4. Oxygen is passed over the cathode and hydrogen over the anode. Hydrogen ions are formed together with electrons at the anode.

Hydrogen ions migrate to the cathode through the electrolyte and electrons produced at the anode flow through an external circuit to the cathode. At the cathode, they are combining with oxygen to form water. The flow of electrons through the external circuit provides the current cell. In order to storage energy, Hydrogen and Oxygen are obtained from water by passing a direct current in a process known as electrolysis. The chemical reactions that take place inside the SOFC and directly involved in the production of electricity are as follows.



Overall cell reaction can be expressed as

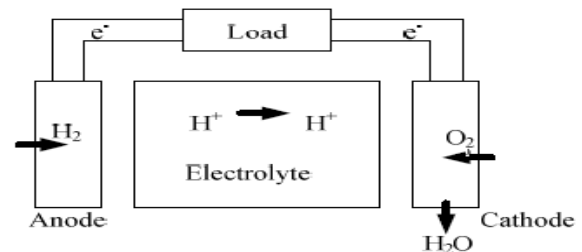
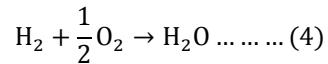


Fig.4 Schematic diagram of a fuel cell

II. DERIVATION OF THE PROPOSED TPTL CONVERTER

Fig. 1 shows the circuit configuration of half-bridge TL converter and conventional full-bridge converter, respectively.

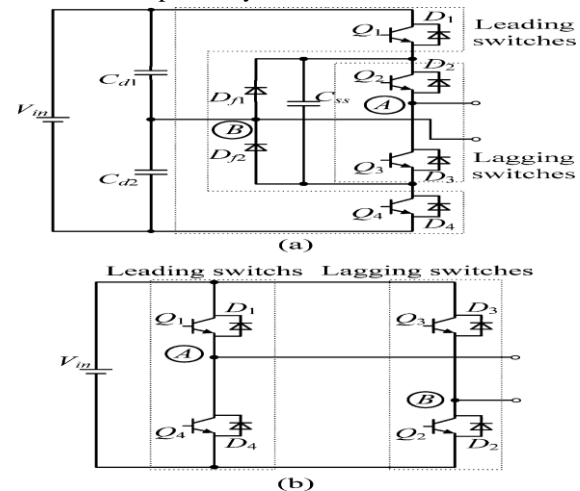


Fig. 5. Comparison of the primary configuration between half-bridge T-converter and full-bridge converter.

(a) Half-bridge TL converter. (b) Full-bridge converter.

For simplicity, only the primary stages are presented. As well known, the two converters can both adopt phase-shifted control, and the switches are classified into the leading switches and the lagging switches as shown in fig.5. The waveforms of v_{AB} and the primary current in two converters are basically the same; therefore, in this sense, the half-bridge TL converter is essentially equivalent to the full-bridge converter.

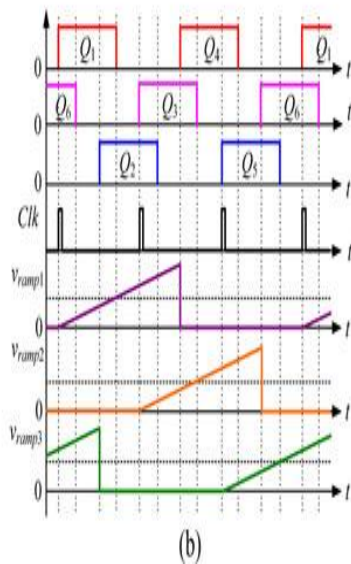
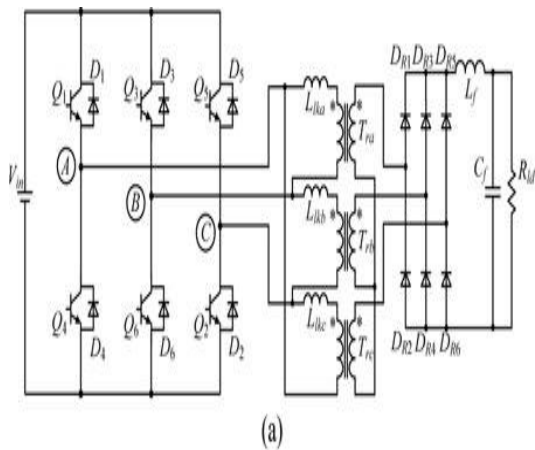


Fig. 6. Topology and control strategy of three-phase full-bridge converter. (a) Main circuit. (b) Control strategy.

Fig. 6(a) shows the topology of three-phase full-bridge converter and the corresponding control strategy, in which a three-phase transformer with Δ -Y connection is employed for the smaller turn's ratios and transformer VA rating. Q_1 , Q_3 , and Q_5 are switched ON in turn according to the rising

edge of the clock signals with interval of one-third switching period; the duty cycles of Q_1 , Q_3 , and Q_5 are modulated by the comparison between three same carrier signals and the error signal. The gate signals of Q_4 , Q_6 , and Q_2 are interleaved with Q_1 , Q_3 , and Q_5 by a half switching period, respectively. For the duty cycles of all the switches are equal, the control strategy in Fig. 3(b) is named as symmetrical duty cycle control. As shown, the three-phase full-bridge converter can be viewed as a combination of two full-bridge sections sharing a common bridge leg.

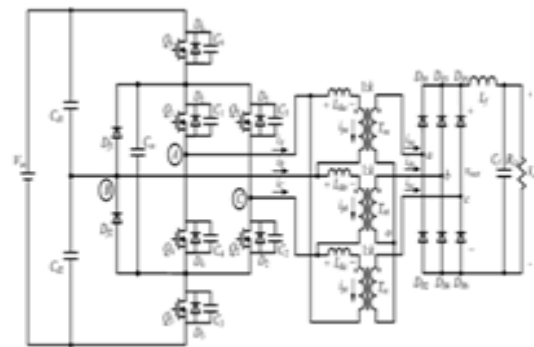


Fig. 7 Proposed TPTL dc/dc converter.

In the full-bridge section composed of Q_1 , Q_3 , Q_4 , and Q_6 , Q_6 is turned ON leading to Q_1 , and Q_3 is turned ON leading to Q_4 , as depicted in Fig. 3(b). According to the correspondence between two converters shown in Fig. 2, the full-bridge section composed of Q_1, Q_3, Q_4 , and Q_6 can be replaced by a half bridge TL section directly, and the transformer and secondary stages remain unchanged. Therefore, a novel TPTL converter can be derived, as shown in Fig. 7. The proposed converter shares the same control strategy shown in Fig. 6(a). As shown in Fig. 7, C_{d1} and C_{d2} are large enough and they share evenly the input voltage, i.e., $V_{Cd1} = V_{Cd2} = V_{in}/2$. L_{lka} , L_{lkb} , and L_{lkc} are the equivalent primary leakage inductances of each phase. D_{f1} and D_{f2} are freewheeling diodes. C_{ss} is the flying capacitor, which is in favor of decoupling the switching transition of Q_1, Q_3, Q_4 , and Q_6 . $D_{R1}-D_{R6}$ are rectifier diodes. The output filter is composed of L_f and C_f , and RL_d is the load.

III. OPERATION PRINCIPLE

This section will analyze the operation principles of the proposed converter. The following assumptions are made for the simplicity before the analysis:

- 1) All power devices and diodes are ideal;

- 2) All capacitors and inductances are ideal;
- 3) the output filter inductance is large enough to be treated as a constant current source during a switching period, and its value equals output current I_o ; and
- 4) L_{lka} , L_{lkb} , and L_{lkc} are identical, and $L_{lka} = L_{lkb} = L_{lkc} = L_{lk}$. Fig.8 shows the key waveforms of the proposed converter; as seen, the converter adopts symmetrical duty cycle control, and each switch has a maximum conduction period of 120° . Evidently, if the duty cycle is less than 0.167, only one switch will turn ON at any moment, and the output voltage will be zero; furthermore, if the duty cycle is beyond 0.33, the output voltage will be uncontrolled, so the required range for the duty cycle of any switch is from 0.167 to 0.33.

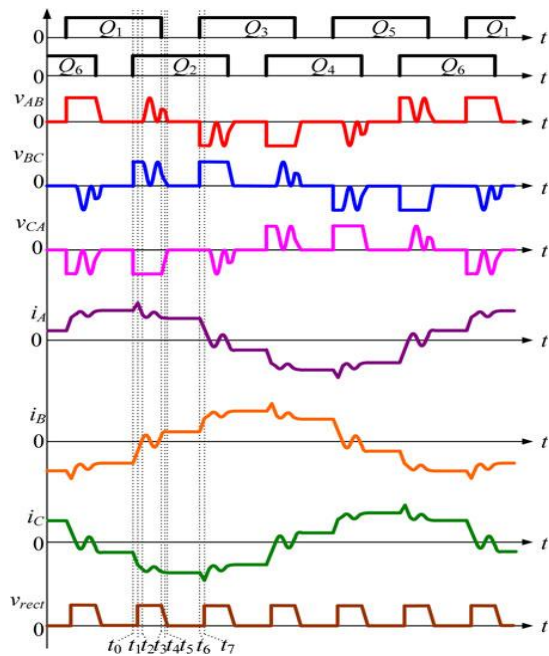
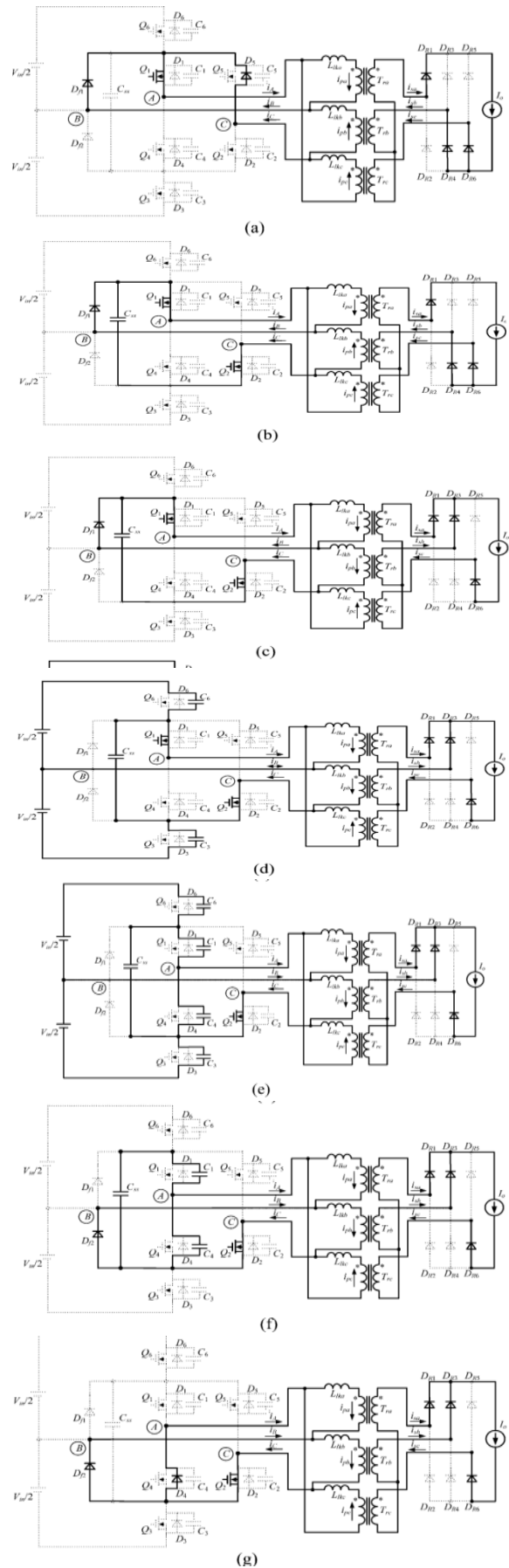


Fig. 8. Key waveforms of the proposed TPTL converter.

There are disparities between several operation principles due to different steady-state operation points and devices parameters of the converter. In this paper, only one specific example will be described due to publication space limitations. Fig. 6 shows eight operation stages of the converter under rated conditions. The other operation stages during the rest of a switching period are not depicted but they are symmetrically equivalent, expect for the fact that they are phase-shifted. The basic equations of the voltages and currents of the transformer are listed as follows:



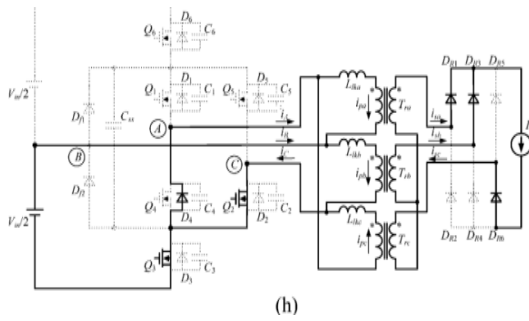


Fig.9. Equivalent circuits under different operation stages. (a) prior to t_0 . (b) $[t_0, t_1]$.(c) $[t_1, t_2]$.(d) $[t_2, t_3]$. (e) $[t_3, t_4]$. (f) $[t_4, t_5]$. (g) $[t_5, t_6]$. (h) $[t_6, t_7]$.

$$v_{AB} + v_{BC} + v_{CA} = 0 \dots \dots \dots (5)$$

$$i_{sa} + i_{sb} + i_{sc} = 0 \dots \dots \dots (6)$$

$$\frac{di_{pa}}{dt} = k \frac{di_{sa}}{dt} = \frac{v_{Llka}}{L_{lk}} \dots \dots \dots (7)$$

$$\frac{di_{pb}}{dt} = k \frac{di_{sb}}{dt} = \frac{v_{Llkb}}{L_{lk}} \dots \dots \dots (8)$$

$$\frac{di_{pc}}{dt} = k \frac{di_{sc}}{dt} = \frac{v_{Llkc}}{L_{lk}} \dots \dots \dots (9)$$

where k represents the secondary-to-primary turns ratios of the transformer. The voltage of leakage inductance of the transformer can be derived from (1)–(4) and is given in the following equation:

$$v_{Llka} + v_{Llkb} + v_{Llkc} = 0 \dots \dots \dots (10)$$

1) Stage 1 [prior to t_0] [see Fig. 9(a)]: Prior to t_0 , Q_1, D_{f1} , and D_5 are conducting in the primary side; the voltages of the transformer windings are zero, so the rectified voltage v_{rect} is zero too.

2) Stage 2 $[t_0, t_1]$ [see Fig. 9(b)]: At t_0 , Q_2 is turned ON with hard-switching condition and the current transfers from D_5 to Q_2 . v_{BC} rises to $V_{in}/2$ while v_{CA} decays to $-V_{in}/2$. In the primary section of the converter, the sum of v_{Llka} and v_{pa} is zero, and the sum of v_{Llkc} and v_{pc} is $-V_{in}/2$. Meanwhile, in the secondary section of the converter, v_{sb} is equal to v_{sc} , and v_{rect} is the difference between v_{sa} and v_{sc} . The secondary current of T_{ra} , i_{sa} , is equal to I_o , so the primary current of T_{ra} , i_{pa} , is constant as kI_o ; then, v_{Llka} is equal to zero. From (5), (6), (10), and the conditions mentioned above, the three-phase line currents i_A, i_B , and i_C can be obtained.

$$i_A(t) = i_A(t_0) + \frac{V_{in}}{2L_{lk}}(t - t_0) \dots \dots (11)$$

$$i_B(t) = i_B(t_0) + \frac{V_{in}}{2L_{lk}}(t - t_0) \dots \dots (12)$$

$$i_C(t) = i_C(t_0) + \frac{V_{in}}{2L_{lk}}(t - t_0) \dots \dots (12)$$

From (7)–(9), i_C decays while i_A and i_B rise linearly. The primary current of transformer-B, i_{pb} , increases with i_B ; when i_{pb} rises to zero, D_{R4} turns OFF and D_{R3} turns ON naturally, in which a commutation process in the secondary stage is completed. 3) Stage 3 $[t_1, t_2]$ [see Fig. 9(c)]: During this stage, $Q_1, Q_2, D_{f1}, D_{R1}, D_{R3}$, and D_{R6} are conducting. Similarly, from (5), (6), (10), and other constraints between voltages.

IV. SIMULATION RESULTS

Here the simulation is carried out by different cases are shown in below by using Matlab/simulink software.

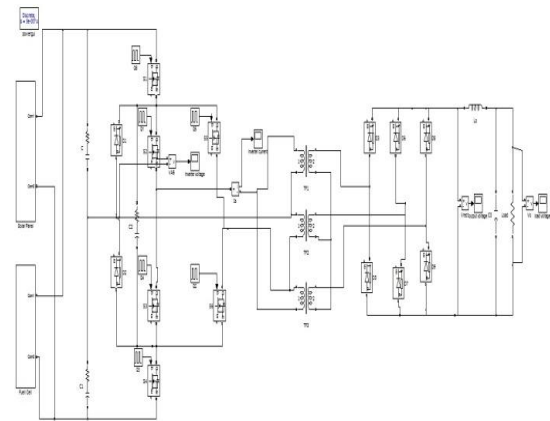


Fig.10. Matlab/simulink model

As shown in the fig. 10, the three phase three level DC/DC converter is connected to the solar and fuel energy sources. The proposed converters are composed of an NPC inverter connected to the primary side of a three-phase high-frequency transformer. The secondary side of the transformer feeds a three-phase rectifier, and the output stage of the converter is composed of the output filter and the load. The symmetrical duty cycle control was adopted in the converter proposed, and the converter has the features including lower voltage stress on switches, soft-switching capabilities, and voltage source characteristic for output stage.

The output waveforms obtained at PV cell and fuel cell are shown in fig.11 and fig.12 respectively.



Fig.11. Output voltage waveform of photovoltaic cell

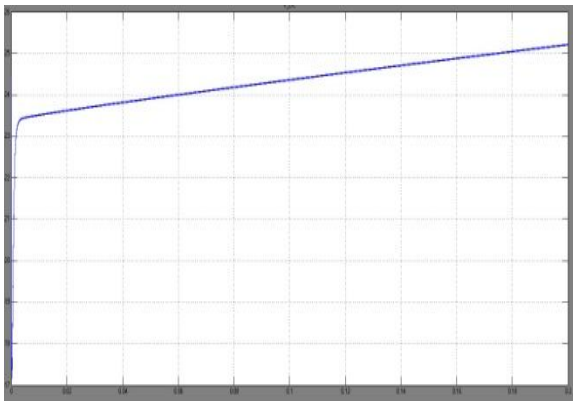


Fig.12 Output voltage waveform of fuel cell

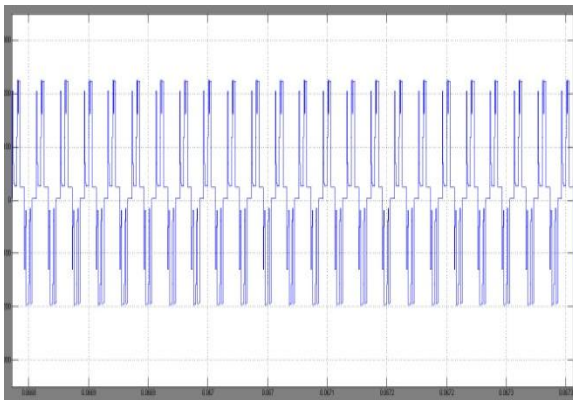


Fig.13. voltage waveforms across inverter

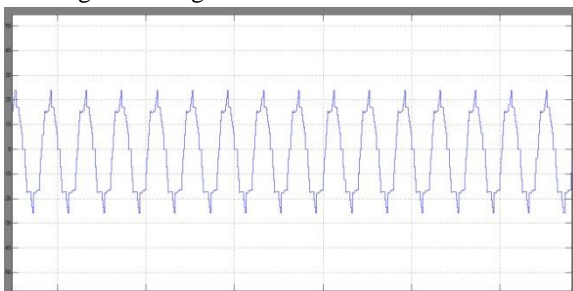


Fig.14. current waveform at inverter output

As shown in the fig.13 and fig.14 the inverter adopting symmetrical duty cycle converts DC input from the sources and produces AC output as shown in fig.15 which is stepped down. Then after the rectifier at the end converts the AC into DC and is then fed to the load. Fig.16 shows the voltage waveform across the load.

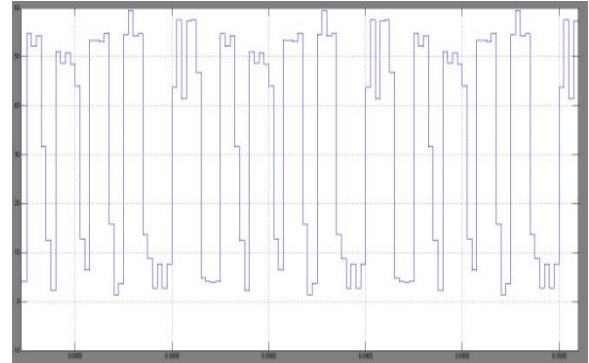


Fig.15. waveforms of Output voltage

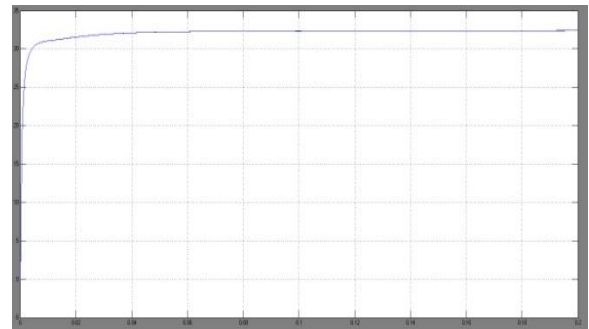


Fig.16. voltage waveform across Load

V. CONCLUSION

A novel ZVS Three-Level DC/DC converter was introduced in this paper. The operation stages and characteristics of the proposed converter were presented. It was shown that this converter reduces the voltage stresses across the main switches to half of the input voltage. Therefore, devices with lower voltage rating, which present better characteristics, can be used. Besides, the addition of a flying capacitor in the primary side allows ZVS operation for all switches with phase-shift control. These characteristics make the proposed converter an interesting option for high voltage, high-power applications that require high efficiency. The proposed converter has a voltage-fed characteristic at the input side, which will lead to a high input current ripple. For the higher switching loss will degrade the performance of the proposed converter,

it is necessary to investigate the improved control schemes in the next step to realize the soft-switching for switches.

REFERENCES

- [1] D. M. Sable and F. C. Lee, "The operation of a full-bridge, zero-voltage switched PWM converter," in *Proc. Virginia Power Electron. Center Semin*, 1989, pp. 92–97.
- [2] X. Ruan and Y. Yan, "Soft-switching techniques for PWM full bridge converters," in *Proc. IEEE Power Electron. Spec. Conf.*, 2000, pp. 634–639.
- [3] P. D. Ziogas, A. R. Prasad, and S. Manias, "Analysis and design of a three phase off-line DC/DC converter with high frequency isolation," in *Proc. IEEE Ind. Appl. Soc. Annu. Meeting*, 1988, pp. 813–820.
- [4] R. W. De Doncker, D. M. Divan, and M. H. Kheraluwala, "A three phase soft-switched high-power-density DC/DC converter for high-power applications," *IEEE Trans. Ind. Appl.*, vol. 27, no. 1, pp. 63–73, Jan./Feb. 1991.
- [5] J. Jacobs, A. Averbeg, and R. De Doncker, "A novel three-phase DC/DC converter for high-power applications," in *Proc. IEEE Power Electron. Spec. Conf.*, 2004, pp. 1861–1867.
- [6] H. Cha and P. Enjeti, "A novel three-phase high power current-fed DC/DC converter with active clamp for fuel cells," in *Proc. IEEE Power Electron. Spec. Conf.*, 2007, pp. 2485–2489.
- [7] A. K. S. Bhat and R. L. Zheng, "A three-phase series-parallel resonant converter-analysis, design, simulation, and experimental results," *IEEE Trans. Ind. Appl.*, vol. 32, no. 4, pp. 951–960, Jul./Aug. 1996.
- [8] A. K. S. Bhat and R. L. Zheng, "Analysis and design of a three-phase LCC type resonant converter," *IEEE Trans. Aerospace. Electron. Syst.*, vol. 34, no. 2, pp. 508–519, Apr. 1998.
- [9] A. Sunil, G. E. Michael, and J. W. Michael, "Analysis and design of a new three-phase LCC-type resonant DC-DC converter with capacitor output filter," in *Proc. IEEE Power Electron. Spec. Conf.*, 2000, pp. 721–728.
- [10] M. Almardy and A. K. S. Bhatt, "Three-phase (LC) (L)-type series resonant converter with capacitive output filter," in *Proc. IEEE Int. Conf. Power Electron. Drive Syst.*, 2007, pp. 468–475.

BIODATA

Author



P. Vijay was born in Nizambad, Telegana state, India in 1988. He received the B.Tech Degree in Electrical and Electronics Engineering from the Jawaharlal Nehru Technological University city, Hyderabad, India in 2011. Now presently going to receive master Degree from the same university where he is pursuing M-Tech. His main research interests include Power electronics drives and three level dc-dc converters and renewable energy generation.

Co-Author



Dr. J. Namratha Manohar is a Doctorate in Electrical Engineering from JNTUH. She has acquired her Bachelor of Engineering (BE) Degree from Osmania University in the year 1982, MCA from IGNOU in the year 2004; M.Tech in the year 2006. She is presently Professor in the Department of Electrical and Electronics Engineering and Dean Academics at Lords Institute of Engineering and Technology, Hyderabad, India. She has a total of 32 years of experience. She has served as Manager at M/S. Hindustan Cables Limited for 17 years in various departments as Quality Control, Engineering and Production Planning and Control. She has 15 years of experience as a Professor. Her research areas include Power System Performance Optimization, FACTS Devices and Neural Networks. She has published about 11 papers and prepared several Manuals.